Theoretical and Applied Fracture Mechanics 121 (2022) 103525

Contents lists available at ScienceDirect

Theoretical and Applied Fracture Mechanics

journal homepage: www.elsevier.com/locate/tafmec

Experimental observations on the effect of thermal treatment on the crack speed and mode I and II fracture toughness in brittle and ductile rocks

Mahmoud Alneasan [a], Abdel Kareem Alzo'ubi [b,*], Mahmoud Behnia [c], Omer Mughieda [b]

[a] Civil Engineering Department, Tishreen University, Latakia, Syria
[b] Civil Engineering Department, Abu Dhabi University, Al Ain, UAE
[c] Department of Mining Engineering, Isfahan University of Technology (IUT), Isfahan 8415683111, Iran

A R T I C L E I N F O

Keywords:
Thermal treatment
Crack propagation speed
Crack acceleration
Fracture toughness
Brittle behaviour
Ductile behaviour

A B S T R A C T

The mechanical properties of rocks are greatly affected by thermal treatment, as this treatment can either improve or worsen these properties depending on the mineralogical composition. Therefore, the effect of thermal treatment on the (1) crack speed properties such as crack propagation speed, crack acceleration, and deceleration, and (2) fracture resistance to grow under two loading modes (pure mode I and pure mode II) was investigated for both brittle and ductile rocks. The ductile type was mudstone, which is a clay-rich rock with a high affinity for water. While the brittle type was granite, which does not contain water-active minerals such as clay or lime. Eighteen semi-circular specimens of mudstone and granite were prepared and tested at room temperature (RT), 250 and 500 °C. The results showed one behavioral trend for the effect of temperature on the mudstone. Due to the drying of clay minerals by increasing the temperature, the crack speed and fracture toughness improved significantly under pure mode I and II after thermal treatment. On the other hand, the thermal treatment of granite caused two behavioral trends. The first trend shows that crack speed and fracture toughness increased under pure mode I and II by increasing the temperature from RT to 250 °C due to crack arrest by randomly distributed thermal microcracks. In the second trend, they decreased below their normal levels under treatment from room temperature to T = 500 °C due to the extension and coalescence of thermal microcracks. The granite behavior changes depending on the density and extension of thermal microcracks. Under the three temperatures of RT, 250, and 500 °C, and for the two rock types, crack propagation speed, crack acceleration, and deceleration under pure mode II were greater than that under pure mode I. Where the fracture goes through three main stages growth, high acceleration, high deceleration, and low deceleration stages. In addition, the effect of temperature on the fracture toughness ratio (K_{IIC}/KIC) was evaluated and the results showed that increasing the temperature increased the fracture toughness ratio. This means that after thermal treatment, the improvement rate of fracture toughness under pure mode II is better than that under pure mode I, and the crack tends to grow under pure mode I rather than mode II.

1. Introduction

Fractures are common in rock masses, as their density, extension, and number increase with increasing the scale of the studied area [1–4]. For small laboratory specimens, the effect of fractures is limited to microcracks. By increasing the size of the area of interest, the effect of flaws, fractures, joint sets, and a network of intersected discontinuities appear and the rock mass becomes weaker. These fractures are mainly subjected to three loading modes, opening mode (pure mode I), sliding mode (pure mode II), and tearing mode (pure mode III). Temperature and thermal stresses affect rock strength in many engineering projects such as rock slopes, geothermal energy, hydraulic fracturing, and nuclear waste burial areas. Fractures in the rock mass grow at various speeds and show different resistance to growth depending on; the rock type, loading mode, and temperature of the rock mass.

Many researchers have investigated the effect of temperature on rock behaviour. Liu and Xu [5] investigated the effect of temperature (room temperature to 1000 °C) on uniaxial compressive strength (UCS) and elastic modulus (E) of marble, they showed that for T less than 400 °C, UCS and E change at different levels with increasing the temperature.

* Corresponding author.
E-mail addresses: mahmoud.alneasan@tishreen.edu.sy (M. Alneasan), abdel.alzoubi@adu.ac.ae (A.K. Alzo'ubi), behnia@cc.iut.ac.ir (M. Behnia), omer.mughieda@adu.ac.ae (O. Mughieda).

https://doi.org/10.1016/j.tafmec.2022.103525
Received 17 May 2022; Received in revised form 30 June 2022; Accepted 1 August 2022
Available online 8 August 2022

While for T greater than 400 °C, UCS and E are inversely proportional to temperature and they decrease linearly with increasing temperature. Zhang, et al. [6] studied the dynamic fracture toughness of marble and gabbro under pure mode I (K_{IC}) for temperatures between 20 and 600 °C. Their results showed that the K_{IC} is temperature-dependent and it decreases with increasing the temperature. Funatsu, et al. [7] conducted experimental tests using notched semi-circular specimens (SCB) and single-edge notched round bar (SENRBB) to investigate the effect of combined temperature and confined pressure on the fracture toughness of the clay-bearing rocks (sandstone and tuff). Results showed that for sandstone, the K_{IC} was approximately constant for T between 25 and 125 °C, while for T greater than 125 °C, the K_{IC} started to increase. For the tuff, the K_{IC} decreased for T between 25 and 75 °C and then started to increase for temperatures greater than 75 °C. Al-Shayea, et al. [8] studied the effect of temperature between 27 and 116 °C on the fracture toughness of limestone under pure mode I and mixed-mode loading I/II and showed the increase of fracture toughness by about 25 % with increasing the temperature from 27 to 116 °C. Kang, et al. [9] used semi-circular specimens to examine the effect of temperature on the fracture toughness of granite under pure mode I, mixed-mode loading I/II, and pure mode II. They showed that by increasing the temperature of thermal treatment from room temperature to 900 °C, fracture toughness under the previous three loading modes decreases by 80.54 %, 86.69 %, and 81.06 %, respectively. In addition, many experimental studies have focused on the effect of temperature on the mechanical properties of different rock types; basalt [10], siltstone [11], dolerite [12], and granite [13], and numerical models for thermally induced damage of rocks; [14–16].

It is noteworthy to mention that there are no direct studies on the effect of temperature on the crack speed properties such as crack propagation speed, crack acceleration, and deceleration, especially in rock fracture mechanics. Most studies focused on the effect of rock type, loading, or strain rate on crack propagation speed. Liu, et al. [17] measured the crack propagation speed in four brittle materials, black sandstone, red sandstone, green sandstone, and BMMA, and concluded that under the same loading conditions, the crack propagation speed and fracture toughness increase with increasing the elastic modulus of brittle material. Liu, et al. [18] investigated the behaviour of fracture induced by blasting from tunnel spandrel and concluded that the rate of dynamic energy release changes during crack propagation, the crack propagation speed is not constant along the fracture path and there are crack arrest points in which the crack velocity is very small. Wan, et al. [19] developed a method to measure the pure mode I fracture toughness under blasting and showed that the propagation toughness is a function of the crack tip speed, the crack propagation speed is not constant during crack propagation and the roughness of fracture surface increases with the increasing the crack propagation speed. Alneasan and Behnia [20] experimentally studied the effect of quasi-static and dynamic strain rates on the crack propagation speed under three loading modes and concluded that the crack propagation speed has its maximum value under pure mode II, by changing the loading mode from mode I to mixed mode I/II and mode II, the crack propagation speed increase. In addition, they concluded that the crack propagation speed increases with increasing strain rate.

Based on the above, the effect of thermal treatment on the crack speed properties is not addressed properly until now and it needs further investigations. In addition, the effect of thermal treatment on the fracture toughness in ductile clay-rich rocks (mudstone) in comparison with brittle rocks (granite that does not have water-active minerals) has not been sufficiently investigated. This study will further our understanding of the mechanical behavior of fractures in thermally treated rocks that have a high affinity for water in terms of the crack speed and fracture toughness under pure mode I and pure mode II of two rock types; mudstone and granite.

2. Mineralogical study

The mineralogical study contributes to determining the scientific name of the rock after determining the main constituent minerals. In addition, it is used to accurately determine grain size distribution and the type of fractures through grains (intragranular fractures) or between grains (intergranular fractures). The mineralogical composition and grain size distribution of granite and mudstone are shown in Fig. 1. The granite used in this study consists of about 25 % quarts, less than5% orthoclase, and about 70 % plagioclase. Based on these percentages and the QAPF diagram for the classification of plutonic rocks (International Union of Geological Surveying IUGS), the scientific name of this rock type is granodiorite. In addition, Fig. 1-d shows that 90 % of the granodiorite in this study consists of grains with sizes between 278 and 1092 μm. The maximum percentage is for grains of size 500 μm. As for the mudstone, the mineralogical composition of this rock type is shown in Fig. 1-b. Gray, white and black colors in this figure indicate clay, calcite, voids, and pores, respectively. The mudstone used in this study consists of about 92 % clay, 6 % calcite, and 1 % pores and voids. Therefore, this rock type represents a clay-rich rock and 90 % of this rock type consists of grains ranging in size between 9 and 28 μm (Fig. 1-e). The maximum percentage is for grains of size 18 μm which are clay-size grains.

3. Experimental study

For each rock type, eighteen semi-circular rock specimens (SCB) were prepared to be tested under three points bending test to investigate the effect of thermal treatment on cracks induced under pure mode I and pure mode II. As shown in Fig. 2, blocks of suitable sizes of mudstone and granite were sought to be homogeneous, free from defects, and taken from the same large block. Then, cores with a diameter of 100 mm were taken from each rock type to be sliced into disks with a thickness of 35 mm. Each disk was then divided into two equal semi-circular specimens by using a blade with a thickness of 2 mm. Taking into account experimental error caused by cutting each circular disk into two SCB specimens due to the blade thickness (t), Kuruppu, et al. [21] indicated that if the thickness of the saw blade used to cut the disks is greater than 0.05D (t/D greater than 0.05), where D is the disk diameter, then the values of the measured radius and the measured notch length should be corrected. t/D in our study is 0.02 and is less than 0.05. Therefore, the experimental error of the measured radius and the measured notch can be ignored. The surfaces of the resulting samples were smoothed and polished from all sides, especially the surface to be used to measure the crack propagation speed. Finally, a notch of 25 mm in length was made by using a 0.5 mm thick blade. For SCB specimens under pure mode I, the notch was aligned with the vertical axis of the sample. While for specimens under pure mode II, the notch was inclined at an angle of 50°with the vertical axis of the sample. The geometric properties of the pure modes I and II were determined depending on the numerical study explained later in section 4.

3.1. Thermal treatment

In this study, SCB specimens were investigated under three temperatures, room temperature, 250 and 500 °C. These temperatures were determined as follows: 5 samples of each rock type were thermally treated at temperatures of 100, 250, 500, 600, and 700 °C for 24 h in the furnace. The temperature of the furnace gradually increased at a constant rate of 4.2 °C per minute to prevent thermal shock. After 24 h, the furnace was turned off and the SCB sample was left to gradually return to the room temperature without thermal shock during the cooling process. After that, the rock samples were taken out of the furnace and carefully examined to monitor color changes and the appearance of thermal cracks. Fig. 3 shows SCB specimens of mudstone and granite after thermal treatment for 24 h under different temperatures. The figure

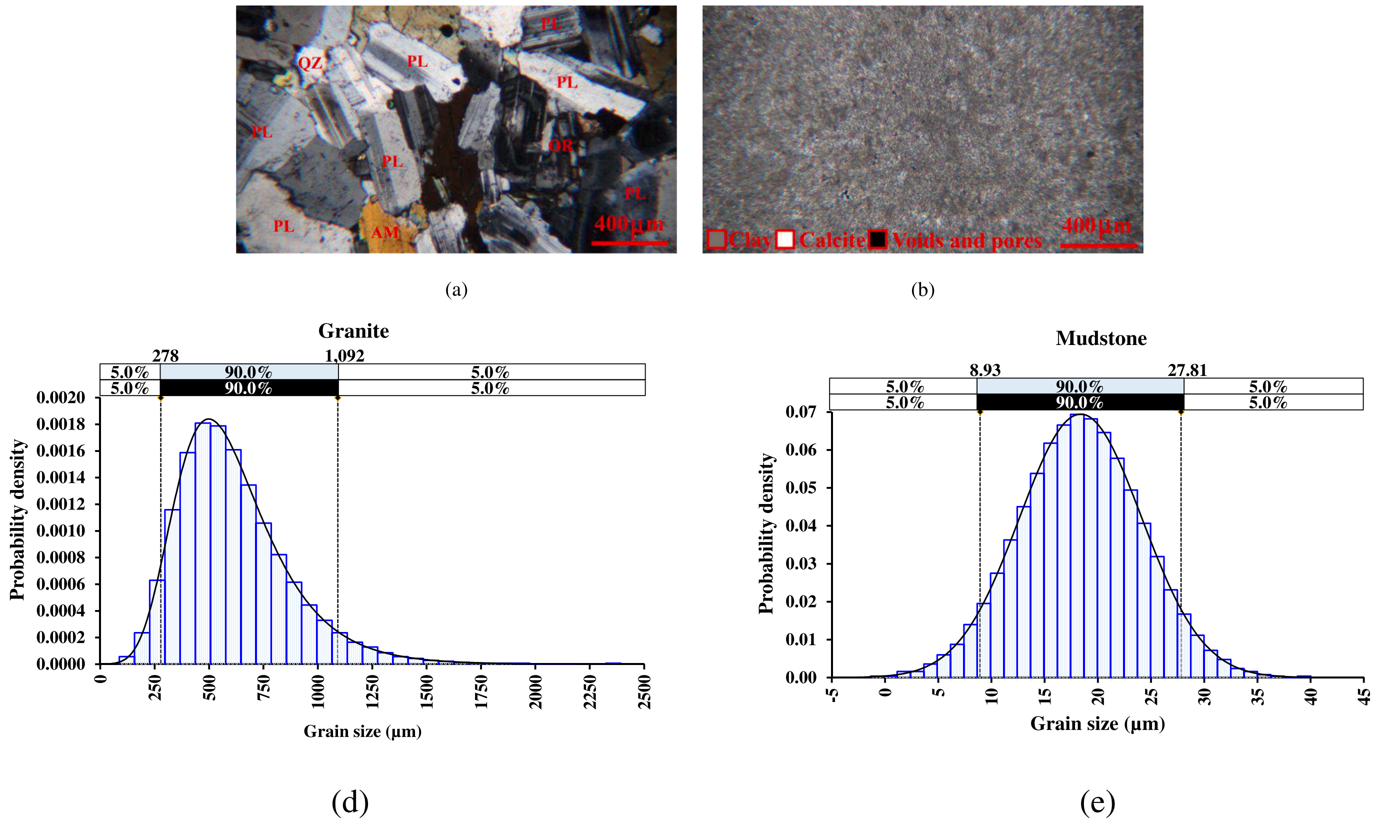

Fig. 1. (a, b) Mineralogical composition of granite and mudstone, respectively, (d, e) grain size distribution of granite and mudstone, respectively. (QZ: quartz, PL: plagioclase, OR, orthoclase, AM: amphibole).

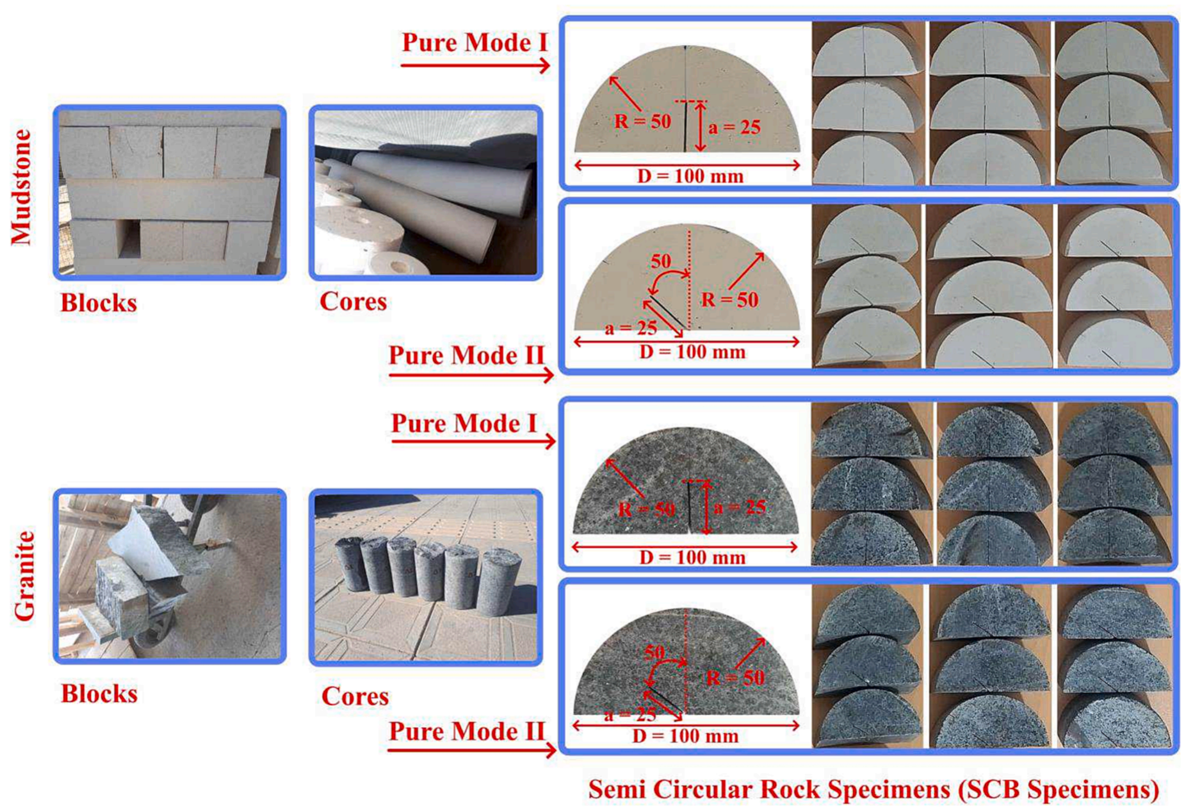

Fig. 2. Preparation of SCB specimens to be tested under three points bending test.

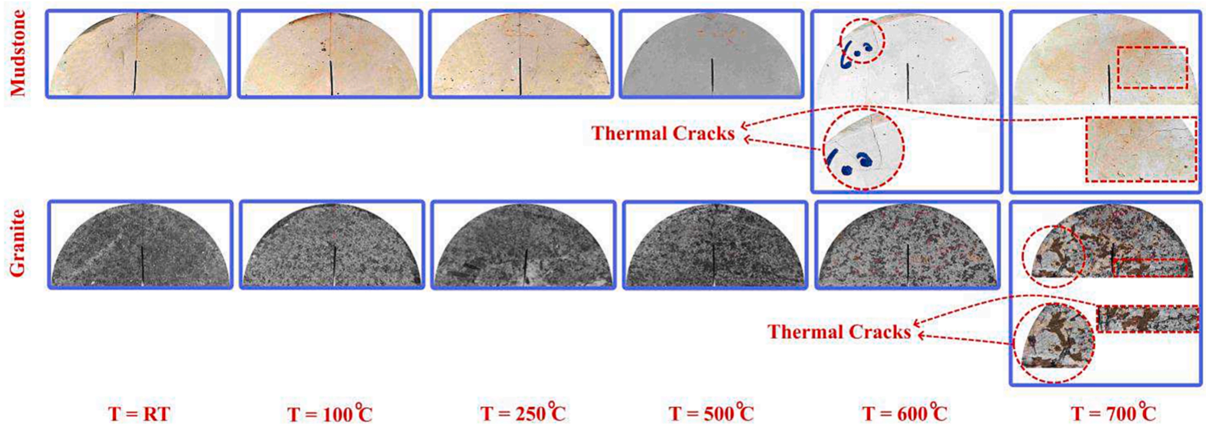

Fig. 3. Thermal treatment of the SCB specimens.

shows that by increasing the temperature of thermal treatment to 500 °C, the color of mudstone changes from beige to gray. While for temperatures greater than 500 °C, the color of mudstone changes to light gray. In addition, Fig. 3 shows that the granite acquires a brown color with increasing temperature, especially for temperatures greater than 500 °C. Moreover, after thermal treatment, no thermal cracks were observed on mudstone samples for temperatures equal to and less than 500 °C. However, for temperatures of 600 and 700 °C, some thermal cracks grew from the sides of the SCB samples. For granite, no thermal cracks were observed for temperatures equal to and less than 600 °C. While once the rock samples were treated with a temperature of 700 °C some thermal cracks in the SCB specimen as shown in Fig. 3. Therefore, it can be concluded that the temperature for the growth of thermal cracks in mudstone and granite (after thermal treatment for 24 h) changes between 500 and 600 °C and 600 to 700 °C, respectively. After the growth of thermal cracks in mudstone and granite, rock samples become very weak and can be crushed by hand. Therefore, the maximum temperature for all the tests of this study was set to be 500 °C which is approximately the maximum temperature at which no thermal cracks were observed on the SCB samples). Two other temperature thresholds were used for testing; room temperature for natural rock before thermal treatment (about 25 °C), and an average temperature between the previous two temperatures (250 °C). Although, the temperature for growth of thermal cracks in granite ranges between 600 and 700 °C, the maximum temperature for original tests was set to 500 °C, as in the mudstone. This is because, for T greater than 573 °C, the α/β transition of quarts occurs. This transition is accompanied by a large extension of specimen volume which in turn increases intergranular stresses, causing the growth of thermal cracks [22]. In addition, Glover, et al. [23] showed depending on the acoustic emission measurements a strong peak of microcracking at α/β transition of quartz due to thermal expansion.

3.2. Experimental procedure

Semi-circular rock specimens of granite and mudstone were tested under pure mode I and pure mode II by using a servo-hydraulic machine of type GOTECH AI-7000 LA 20 with a vertical displacement speed of 1 mm/min. Taking into account that the height of the SCB specimen is 50 mm, therefore, the induced strain rate in these specimens is 7×10^{-4} S^{-1}, which is in the range of the quasi-static strain rate. The system used in this study for measuring fracture toughness and crack propagation speed is shown in Fig. 4. Crack propagation speed was measured in this study by using a method developed by Alneasan and Behnia [20], Alneasan and Behnia [24]. This method mainly depends on the use of conductive copper tapes, which are glued to the sample surface after smoothing and polishing this surface. As shown in Figs. 4, 4 copper tapes were successively glued to one of the sample surfaces. Once the stress intensity factor at the crack tip reaches the fracture toughness of the material, the notch begins to grow and the new fracture cuts these tapes one by one. These tapes are connected to a power supply and digital oscilloscope to determine the cut off time. By measuring the cut off time and the length of fracture between every-two successive tapes, crack propagation speed can be computed and as a result, crack acceleration can also be computed. The first tape was directly glued at the notch tip. The cut off time of this tape approximately corresponds to the fracture initiation

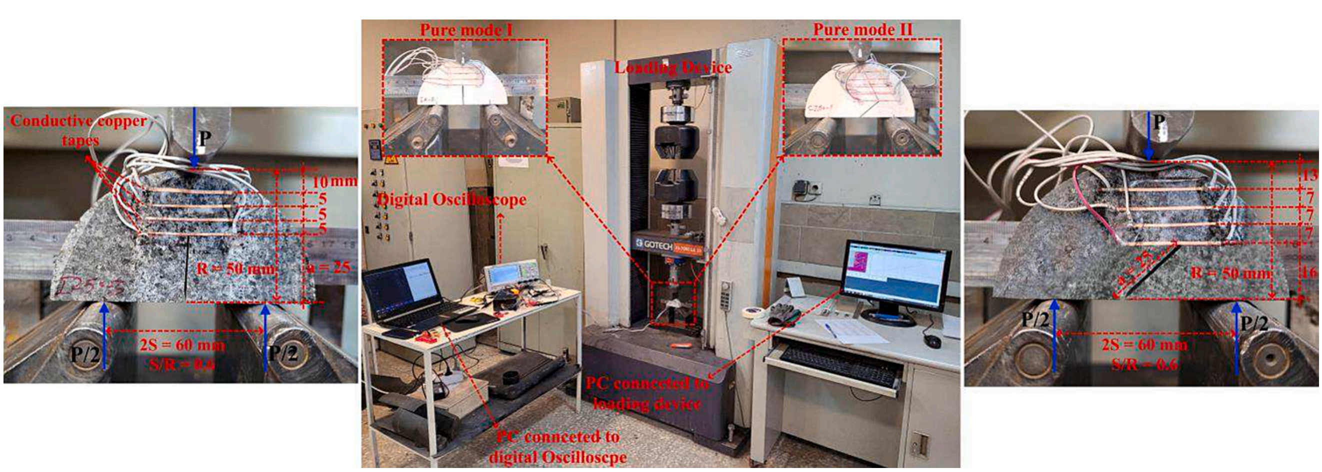

Fig. 4. Loading device and crack propagation speed system of this study.

time. Under pure mode I, the second, third, and fourth tapes were glued at distances of 5, 10, and 15 mm, respectively, from the notch tip. Under pure mode II, due to the inclined notch at an angle of 50°, the distance between copper tapes is different compared to the pure mode I case. The second, third, and fourth tapes were glued at distances of 7, 14, and 21 mm, respectively, from the notch tip The distance between the last tape and the specimen surface where the load was applied was about 10 and 13 mm under pure mode I and pure mode II, respectively. It should be noted that for the calculation of the crack propagation speed, the real fracture length was measured between each two successive copper tapes after the test, and this length was used to calculate the crack propagation speed, not the distance between copper tapes that is shown in Fig. 4. This is because the fracture may deviate from its straight path due to the effect of the loading mode and grain size. In addition, it should be noted that the whole fracture process of SCB specimen occurs in a very short time. Therefore, we must use high sampling rate instruments to measure the cut off time. The digital oscilloscope used in this study is of a type RIGOL DS1054Z and it can detect the cut off time in a very short time due to its high sampling rate which is 1 GSa/*sec*.

4. Numerical implementation

To calculate stress intensity factors and fracture toughness in the SCB specimens under pure mode I and pure mode II, the three points bending test was numerically simulated depending on the displacement discontinuity method (DDM). This method is a branch of the boundary element method (BEM) which was developed by Crouch, et al. [25]. Compared with other numerical methods such as the finite element method (FEM) and finite difference method (FDM), as shown in Fig. 5, in the DDM only the boundaries and discontinuities of the problem are divided into small elements. While in other methods such as FEM and FDM, the entire area must be divided into small elements. Therefore, the number of elements and algebraic equations in the DDM is much less than that in the FEM and FDM, which in turn reduces the size of the data and the time required to solve the problem [26]. A two-dimensional crack propagation code (TDCPC) was used in this study to simulate three points bending test on semi-circular rock specimens. This code was previously developed by Alneasan, et al. [27] to predict crack propagation path in the SCB specimens of brittle materials such as rocks under mixed-mode loading and it was verified depending on numerical (FEM) and experimental results of Ayatollahi, et al. [28]. The stress intensity factors and crack propagation path were computed and predicted depending on the TDCPC and compared with the numerical and experimental results of Ayatollahi, et al. [28]. Depending on this code, the SCB specimen is divided into N DDM elements, about 250 elements for geometry and dimensions of the SCB specimen in this study. Then boundary conditions are defined for these elements. For the top element, this element is defined as a loaded element with $\sigma_n = P$ and $\sigma_s = 0.0$. The supported elements, these elements are defined as two roller bottom supports with vertical displacement equal to zero ($u_n = 0.0$). For other elements, these

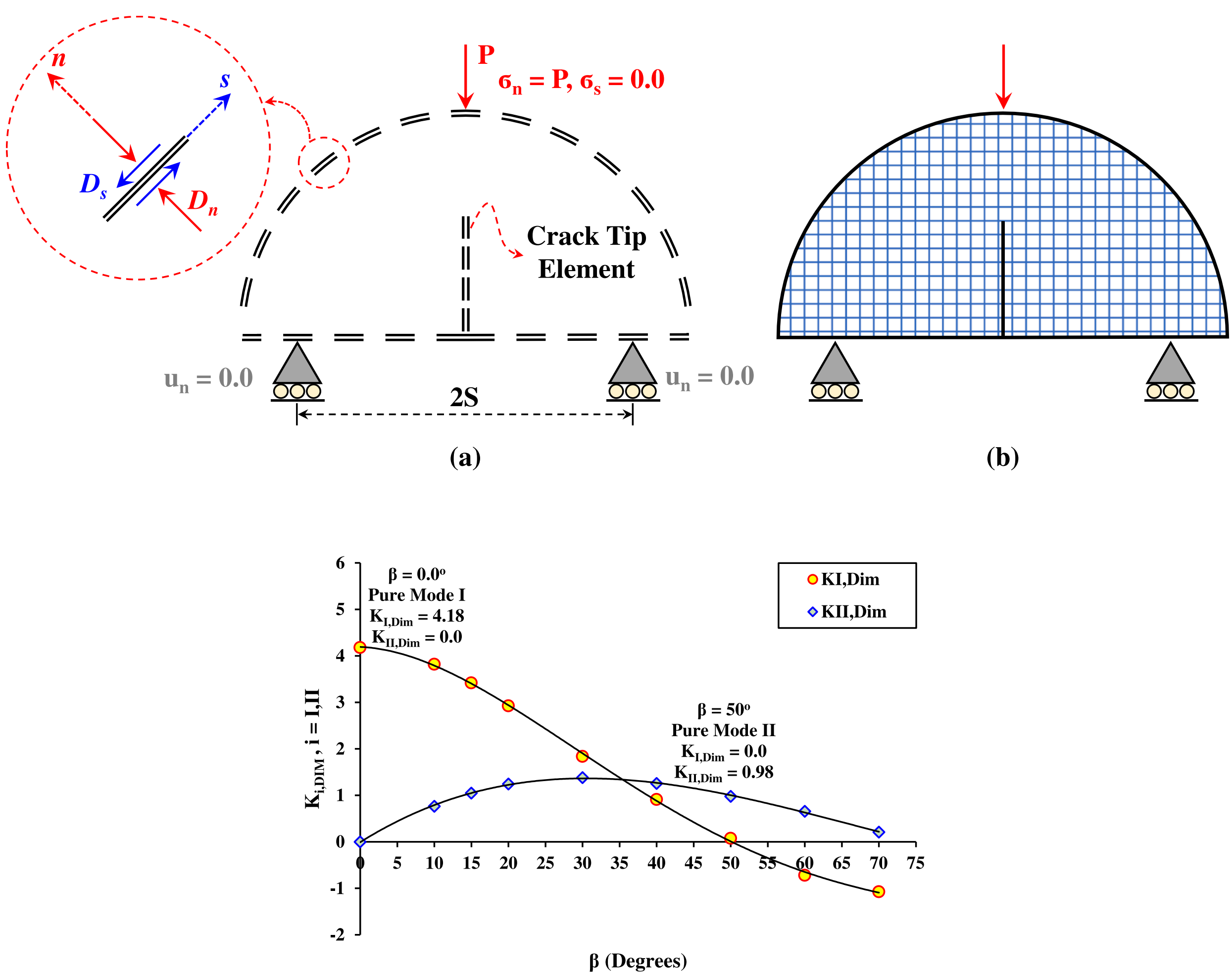

(c)

Fig. 5. Modeling of three points bending test depending on (a) displacement discontinuity method and (b) other methods such as finite element method or finite difference method, (c) dimensionless stress intensity factors as a function of crack inclination angle.

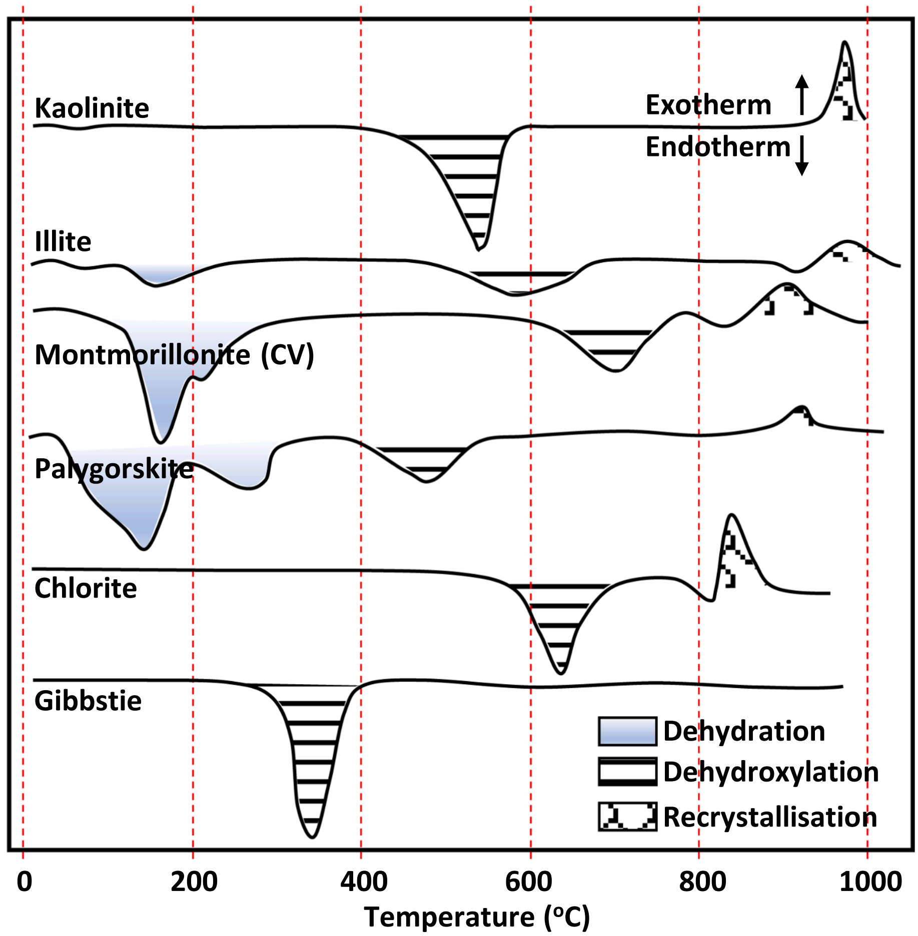

Fig. 6. Representative differential thermal analysis (DTA) curves for common clay minerals and Gibbsite (modified after Cook [29]).

elements are free of any restrictions. When the code runs, firstly the geometry of the model is defined, such as the length, inclination, center coordinates, etc. Then the previously mentioned boundary conditions for loaded elements, bottom supports, and other elements are defined. After that influence coefficients are calculated. These coefficients correlate between boundary conditions and displacement discontinuities (D_n and D_s) which must be calculated by solving a system of algebraic equations. Finally, stress intensity factors of the crack tip element are obtained depending on the displacement discontinuities of this element. For the geometry of the SCB specimen shown in Fig. 2, the distance between the two bottom supports was set to 60 mm (S/R = 0.6), and the crack inclination angle was changed between 0.0 and 60°. Dimensionless stress intensity factors versus crack inclination angle are shown in Fig. 5-c. This figure shows that pure mode I and pure mode II correspond to crack inclination angles of 0.0 and 50°, respectively. Fracture toughness under pure mode I and pure mode II can be calculated depending on:

$$K_{ic} = \frac{P_{cr}}{2RT} K_{i,Dim} \sqrt{\pi a}\,(i = I, II) \tag{1}$$

where P_{cr} is the fracture load and can be obtained experimentally from the displacement-load curve. R, T, and a are the radius, thickness, and notch length, respectively. $K_{i,Dim}$ are dimensionless stress intensity factors.

5. Results and discussions

The results of this study include two parts; the first part discusses the effect of temperature on the velocity properties such as crack propagation speed, crack acceleration, and crack deceleration. And the second one discusses the effect of temperature on the fracture resistance to grow such as fracture toughness under pure mode I, fracture toughness under pure mode II, and fracture toughness ratio (K_{IIC}/K_{IC}).

5.1. *Crack propagation speed and crack acceleration of mudstone*

Crack propagation speed and crack acceleration measured in this study correspond to the average value of these two parameters between every-two successive tapes. This is because the crack propagation speed and crack acceleration were calculated depending on the cut off time of each two successive tapes (CPS = ΔS/ΔT (m/s), CAC = ΔCPS/ΔT (Km/s^2)). Crack acceleration was shown in Km/s^2 because it has very large values, especially under pure mode II. Crack propagation speed and crack acceleration of mudstone under pure mode I and pure mode II are shown in Fig. 7. The main results presented in this figure can be summarized as follow:

1- The crack propagation speed and crack acceleration in the mudstone under pure mode I and pure mode II increase with increasing the temperature. By increasing the temperature from the room temperature to 500 °C, the maximum crack propagation speed under pure mode I and pure mode II, which corresponds to the average speed between the first two successive tapes, increases by 6.5 and 2 orders in magnitude, respectively. Whereas, the maximum crack acceleration between the first two tapes under pure mode I and pure mode II increases by 37 and 4.1 orders in magnitude. As will be shown later in section 5.3.1, clay minerals that constitute 92 % of the mudstone used in this study are greatly affected by the temperature of thermal

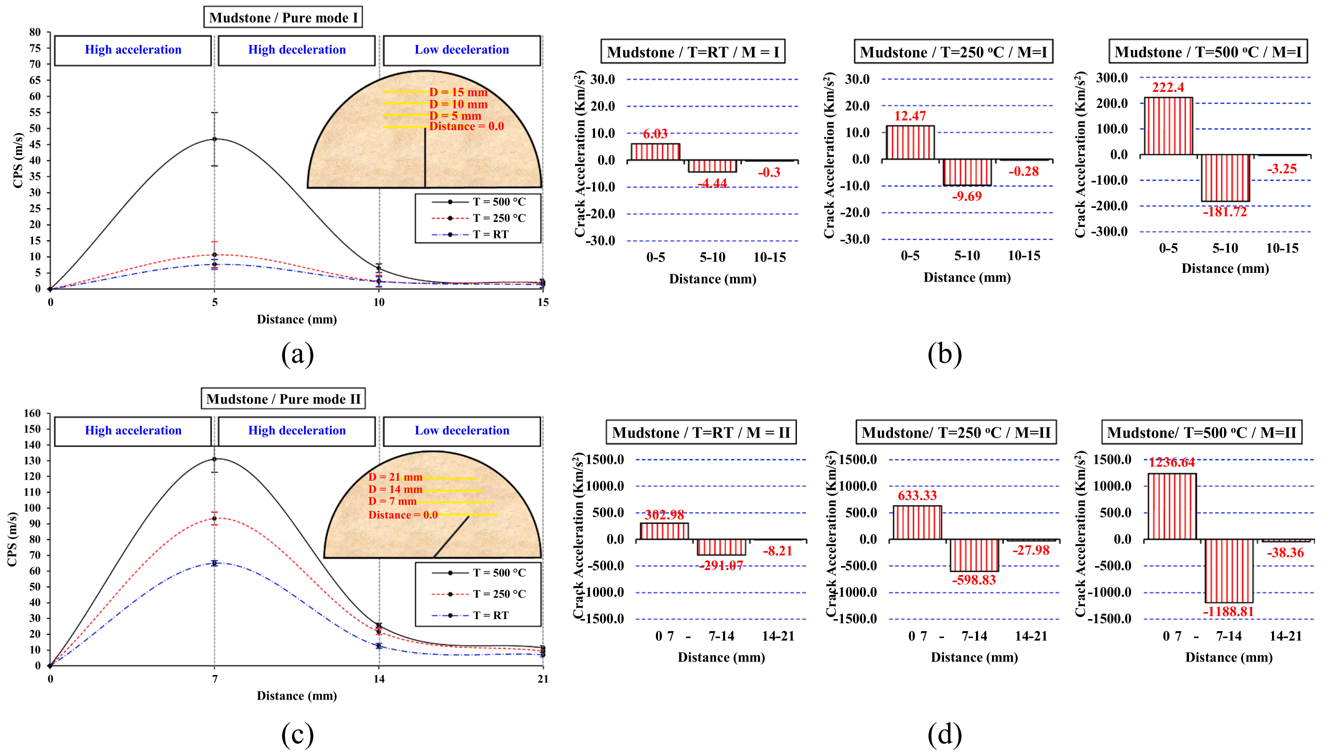

Fig. 7. (a) and (c) crack propagation speed in the mudstone under pure mode I and pure mode II, respectively, (b) and (d) crack acceleration in the mudstone under pure mode I and pure mode II, respectively.

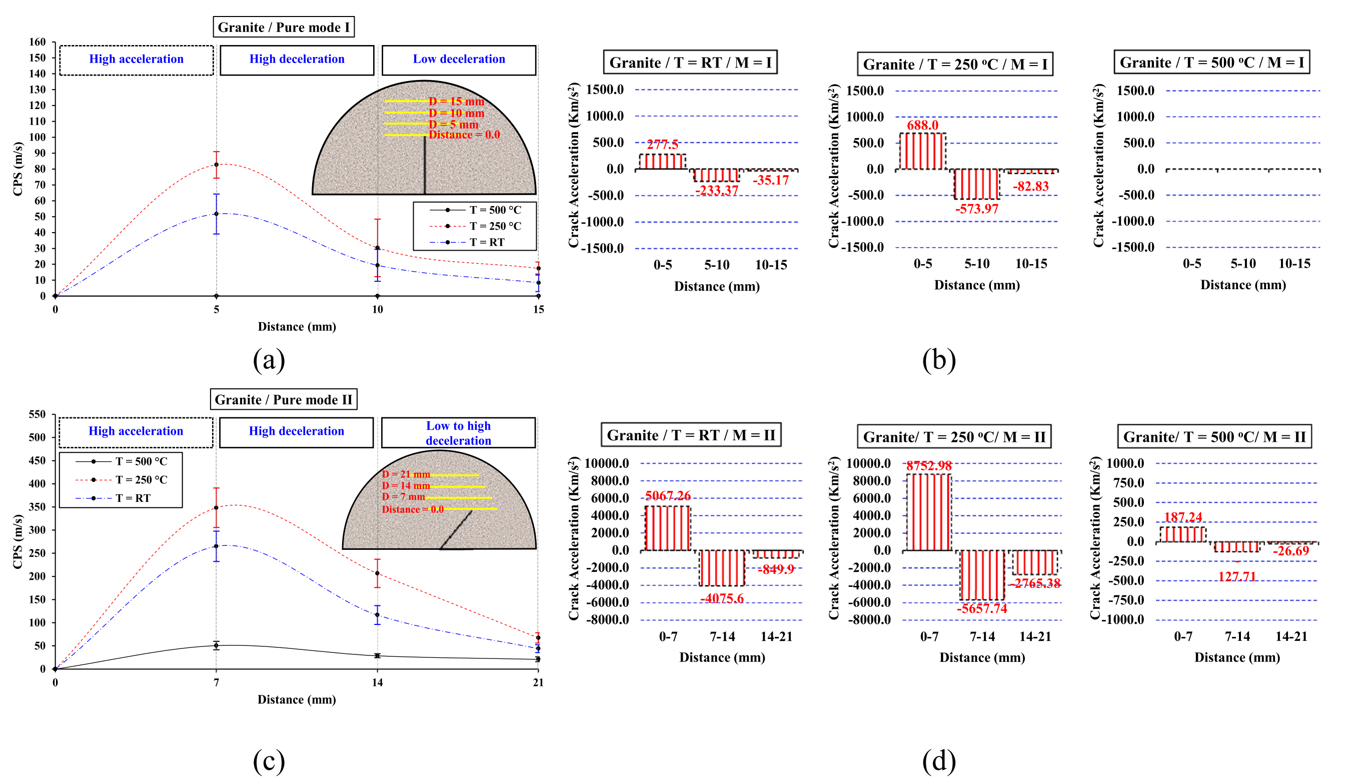

Fig. 8. (a) and (c) crack propagation speed in the granite under pure mode I and pure mode II, respectively, (b) and (d) crack acceleration in the granite under pure mode I and pure mode II, respectively.

treatment. These minerals lose water between their layers during thermal treatment through dehydration and dihydroxylation processes, which causes a decline in the plastic behavior of the material. Therefore, the material becomes stronger and the area under the displacement - load curves, shown later in Fig. 9, increases. An increase in this area means an increase in the strain energy stored in

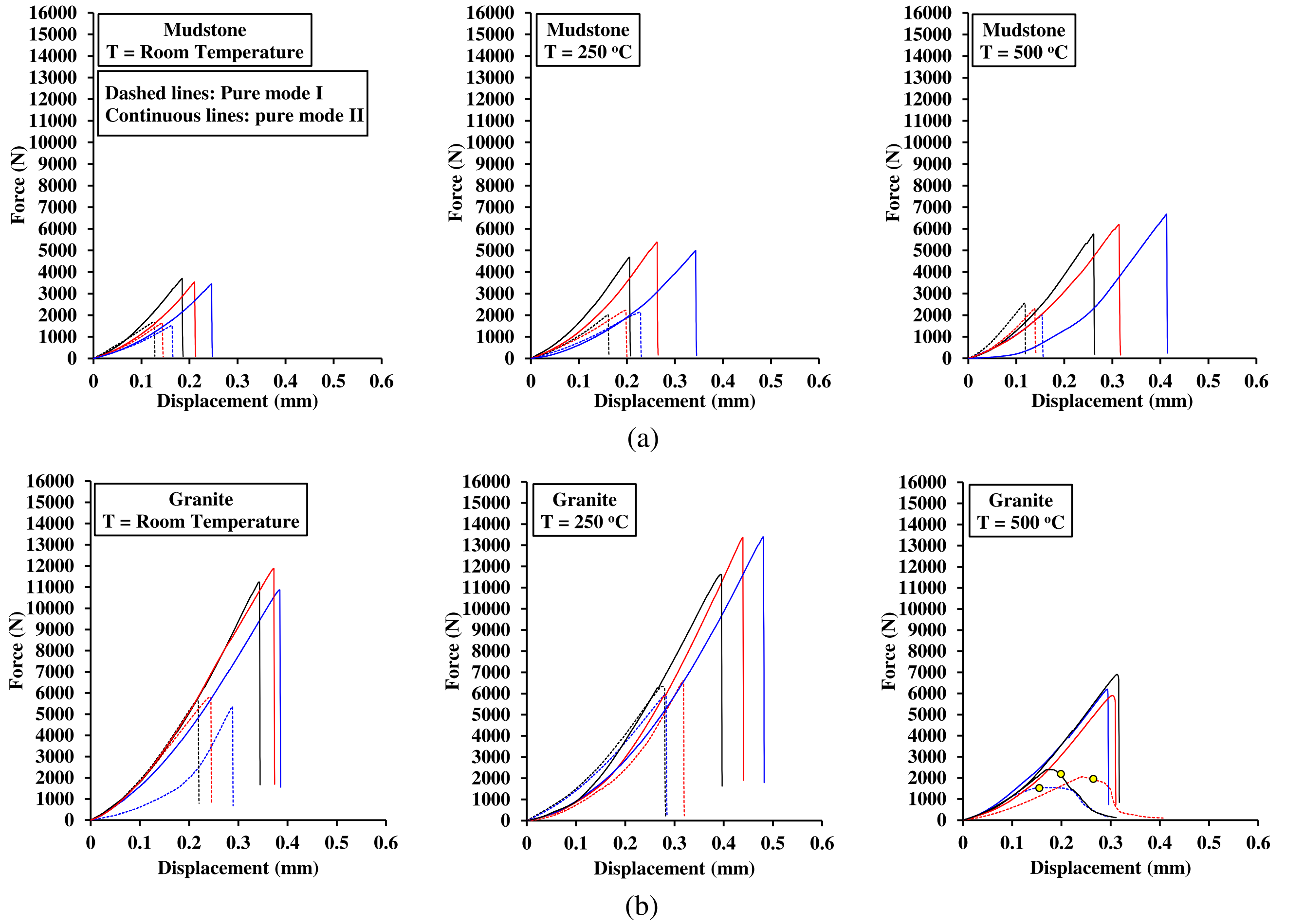

Fig. 9. Displacement-load curves in (a) mudstone and (b) granite under pure mode I and pure mode II for the three temperatures of (RT, 250, and 500 °C), continuous and dashed lines represent pure mode I and pure mode II, respectively.

the rock sample before the moment of fracture. At the moment of fracture, the more strain energy stored in the rock sample, the faster it is released during crack propagation, and thus the faster crack propagation speed. The temperatures that cause a decline in the plastic behavior of clay minerals due to dehydration, dehydroxylation, and recrystallization processes are determined by the clay mineral structure and composition. The effect of temperature on the various common clay minerals is shown in Fig. 6 [29]. Cook [29], Snellings, et al. [30] indicated that optimal activation of the clay minerals is attained through amorphization upon complete dihydroxylation of the octahedral sheet. Depending on Fig. 6, dihydroxylation of most common clay minerals such as kaolinite, illite, montmorillonite, palygorskite, and chlorite can occur at temperatures between 300 and 800 °C. Increasing the temperature to more than 800 °C, can lead to the recrystallization of clay minerals.

2- Crack propagation speed is not constant along the crack path. The crack accelerates and decelerates significantly during growth. According to that, the growth stage is divided into three basic stages, high acceleration, high deceleration, and low deceleration stages. As shown in Fig. 7-a,c, just moments before fracture begins (D = 0.0 mm), the crack is stationary (CPS = 0.0 m/s) and the potential energy stored in the rock sample is maximum. At the moment of fracturing, a quick release of the stored energy occurred and as a result, the crack greatly accelerates to reach the maximum velocity at the first copper tape. Away from the crack tip, between the second and third tapes, the crack decelerates greatly reaching an approximately constant velocity as the majority of energy is already consumed in creating the initial fracture. Moving further from the tip of the notch variable velocity through low deceleration between the third and fourth copper tapes was observed. It can be noted that under pure mode I and pure mode II and for the three temperatures (T = RT, 250, and 500 °C), the maximum crack acceleration is about 10 to 30 % greater than the maximum crack deceleration as shown in Fig. 7-b,d.

3- Crack propagation speed, crack acceleration, and crack deceleration under pure mode II are greater than that under pure mode I. For room temperature, 250 and 500 °C, the maximum CPS under pure mode II is 8.6, 8.7, and 2.8 times greater than that under pure mode I. As will be shown later, fracture load under pure mode II is greater than that under pure mode I. Therefore, the stored energy in the rock sample under pure mode II is greater than that under pure mode I, and as a result, the release of a large amount of energy under pure mode II compared to pure mode I causes a significant increase in the crack propagation speed and acceleration. In other words, the energy required to create pure mode I crack is lesser than the energy required to generate pure mode II crack [31].

5.2. *Crack propagation speed and crack acceleration in the granite*

Similar to the previous section, the crack propagation speed and crack acceleration in granite under pure mode I and pure mode II are shown in Fig. 8. The main difference between the mudstone and granite is that by increasing the temperature of thermal treatment from the room temperature to 250 and then to 500 °C, the crack propagation speed, crack acceleration and crack deceleration in the mudstone increase and their maximum values correspond to T = 500 °C. While in the granite, these parameters increase by increasing the temperature of thermal treatment up to 250 °C. For T = 500 °C, the crack grows so slowly, 0.005 m/s, under pure mode I to the extent that the crack growth in some specimens was observed by the naked eye. The fracture under pure mode I and T = 500 °C loses its brittle behavior and becomes more ductile and the energy stored in the sample before fracture initiation is slowly released during the crack growth stages. Therefore, the crack propagation speed under pure mode I was very low and almost constant, without noticeable values of acceleration and deceleration (see Fig. 8-b under T = 500 °C). For T = 500 °C and pure mode II, the fracture behaviour is more brittle than that under pure mode I with reasonable values of the crack propagation speed, crack acceleration, and crack delectation.

In addition to the above, by comparing the results obtained from the mudstone and granite, the crack propagation speed, crack acceleration, and crack deceleration in the granite under the room temperature and 250 °C are greater than that in the mudstone. Moreover, the results showed that for T = 250 °C, the maximum crack propagation speed in the granite under pure mode I and pure mode II is 1.77 and 2.66 times greater than that in the mudstone, respectively. An important point can be noted in Fig. 8-c for T = RT and 250 °C, the crack deceleration for the last crack propagation stage (14–21 mm) under pure mode II is high compared to its magnitudes under pure mode I in Fig. 8-a. Therefore, it can be said that for granite specimens under pure mode II and T = RT and 250 °C, the energy stored in the rock sample is quickly released due to the high acceleration and deceleration of the fracture from the first to last stage (0–21 mm). While under pure mode I, the energy is quickly released only within the first and second stages (0–10 mm) and the fracture becomes more stable with low acceleration at the last stage (10–15 mm).

Depending on the crack propagation speed measured in the SCB specimens of mudstone and granite, our results indicated three main stages, high acceleration, high deceleration, and low to high deceleration stages. Previous experimental investigations about crack acceleration are rather limited, especially those related to rocks. Arakawa, et al. [32] measured crack propagation speed in single-edge-notched (SEN) specimens of PMMA and they obtained three distinct stages of crack acceleration, deceleration, and re-acceleration as a crack propagated between two circular holes. In addition, Takahashi and Arakawa [33] and Arakawa and Takahashi [34] exhibited crack acceleration and deceleration in one fracture process in PMMA, epoxy, and Homalite-100 specimens. Our results indicated high values of crack acceleration and deceleration as crack propagated in the SCB specimens of mudstone and granite, which are of the order of 10^{+2} to 10^{+7} m/s^2. It is worth mentioning that our results of crack acceleration and deceleration are close those reported by Arakawa, et al. [32], where their results indicated that the maximum crack acceleration or decelartion is of the order of 10^{+6} m/s^2.

5.3. Fracture toughness

Fracture toughness which determines crack resistance to growth is an important parameter in rock fracture mechanics. This parameter is influenced by the loading mode and temperature of thermal treatment [35]. However, the effect of thermal treatment on fracture toughness needs further understanding and it might vary according to the rock type and the main constituent minerals. As shown in section 2, the mineralogical composition of the mudstone is completely different from that of the granite. The main constituent minerals in mudstone and granite are clay and plagioclase, respectively. The fracture toughness of mudstone and granite under pure mode I and pure mode II for the three temperatures (RT, 250, and 500 °C) was computed depending on equation (1). Fracture load P_{cr} was obtained from the displacement-load curve as shown in Fig. 9. To facilitate comparison between the results, all displacement-load curves are shown in the same horizontal and vertical scale. The area under these curves, more accurately under the strain–-stress curves, corresponds to the energy stored in the rock sample before the moment of fracture. Fig. 9 shows that all curves have a distinct peak except those associated with granite samples under pure mode I and thermal temperature of 500 °C, which were marked with yellow circles in Fig. 9-b to show the selected P_{cr}. The existence of this distinct peak indicates the brittle behavior of the material.

Moreover, Fig. 9 shows that by increasing the temperature of thermal treatment from RT to 500 °C under pure mode I and pure mode II in the mudstone, and from RT to 250 °C under pure mode I and II in granite, the peak of displacement-load curves which corresponds to the fracture load and the area beneath these curves increase. This increase in the fracture load causes the increase of the fracture toughness as suggested by Equation (1), and the increase of the area under strain–stress curves causes the increase of the energy stored in the rock sample and this increased the crack propagation speed.

The curves marked with yellow circles in Fig. 9-b indicate that SCB specimens of granite under pure mode I and thermal temperature of 500 °C behave in a ductile manner. No distinct peak was identified and large displacements were recorded in the post-peak behavior. The brittle behavior of the material and the sudden drop of the curve after the peak show the quick release of the stored energy in the rock sample and this caused a great acceleration of the crack. While the ductile behavior of the material and gradual slope of the strain–stress curve after fracture indicates that the energy stored in the rock sample was gradually released during crack growth stages at very low speeds. Therefore, the crack propagation speed, crack acceleration, and deceleration of granite samples under pure mode I and temperature of 500 °C were very low (Fig. 8-a,b). Fig. 9-b under T = 500 °C clearly shows that the loading mode directly affects the fracture behavior. For the same thermal treatment conditions, this figure shows that fractures under pure mode II have a distinct peak and behave in a brittle manner, and vice is versa for fractures under pure mode I. This point was not observed in the fracture behaviour of mudstone because there is only one regime for the effect of temperature on this rock type; improving of rock properties with an increase in temperature due to the drying of clay minerals. Therefore, all displacement-load curves of mudstone have the same trend under the three temperatures. While in granite, there are two regimes for the effect of temperature on this rock type; improving rock properties for T between RT and 250 °C, and then rock properties decrease for T between 250 and 500 °C. Considering that the rock samples containing mode II fractures are stronger and more brittle than those containing mode I fractures [36,37], the weak behavior of the fracture with no distinct peak was only observed under pure mode I. This mechanical behavior between claystone and granite was explained based on the experiments performed in our study. This issue needs further research and expansion of the experimental program to obtain more data about the behavior of these two rock types, which is what we recommend for future research in this field.

5.3.1. Temperature dependence of fracture toughness of mudstone

Fracture toughness under pure mode I (K_{IC}) and pure mode II (K_{IIC}) and fracture toughness ratio (K_{IIC}/K_{IC}) in the mudstone and granite versus the temperature of thermal treatment are shown in Fig. 10. This figure shows that by increasing the temperature of thermal treatment from room temperature to 500 °C in the mudstone (Fig. 10-a), the average value of K_{IC} and K_{IIC} increase by 47 % and 74 %, respectively. Therefore, it can be concluded that the mudstone improves significantly during thermal treatment. This improvement caused an increase in the peak load, energy stored in the rock sample, fracture toughness, and crack propagation speed. Clays that form 90 % of the mudstone have a great affinity for water due to the formation of the diffuse double layer around the negatively charged minerals. Therefore, the fracture toughness of the mudstone increased significantly after thermal treatment due to the drying of clay minerals through two processes, dehydration and dihydroxylation. The dehydration process can occur at temperatures between 100 and 200 °C. In this process, the pore, adsorbed and interlayer water is removed from the rock sample. The dihydroxylation

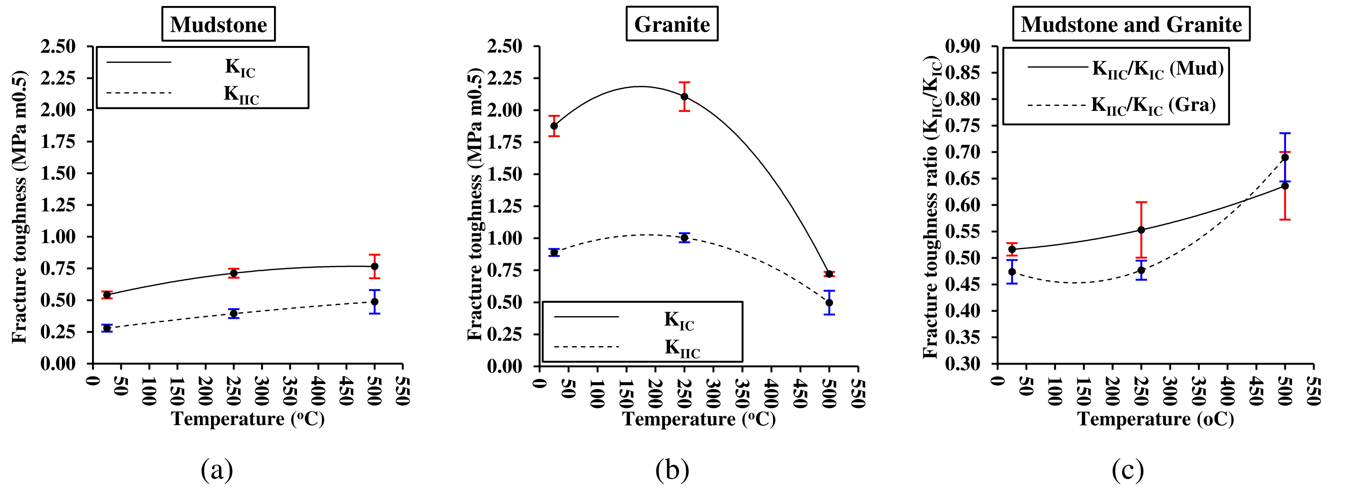

Fig. 10. Fracture toughness in (a) mudstone and (b) granite under pure mode I and pure mode II, (c) the ratio of fracture toughness in mudstone and granite.

process includes the ejection of hydroxyl ions from the crystal structure of the clay minerals at temperatures between 500 and 1000 °C [38,39]. For various common clay minerals such as kaolinite, illite, montmorillonite, palygorskite, and chlorite, Cook [29], Snellings, et al. [30] indicated that dihydroxylation process can occur at a temperature between 300 and 800 °C. This causes complete drying of the rock sample and generates localized tensile stress inside the sample, that in turn leads to the growth of thermal cracks which were observed in the thermally treated specimens at a temperature of 600 and 700 °C (Fig. 3). In general, clay minerals lose their plasticity when the temperature exceeds the limit of the dehydration process but below the limit of the dihydroxylation process, where clay minerals lose hydration, adsorbed, and lattice water [40]. Therefore, as a result of the loss of plasticity during the dehydration process, voids and pores in the rock sample change and the interlayer spaces collapse. On the other hand, when the temperature exceeds the limit of the dihydroxylation process, the layer structures of clay minerals are destroyed.

5.3.2. Temperature dependence of fracture toughness of granite

Fig. 10-b shows two regimes for the effect of temperature on the fracture toughness of granite. The first one shows that by increasing the temperature of thermal treatment from room temperature to 250 °C, the average value of K_{IC} and K_{IIC} increases by 12 % and 13 %, respectively. While the second regime shows that by increasing the temperature from 250 °C to 500 °C, the fracture toughness drops below its normal levels under room temperature, where the K_{IC} and K_{IIC} are equivalent to 38 % and 56 %, respectively, of the fracture toughness under room temperature. Therefore, the thermal treatment improves the properties of the granite used in this study up to 250 °C. Compared with the results of crack propagation speed, we find a complete agreement between the effect of thermal treatment on fracture toughness and crack propagation speed. In the first regime (RT to 250 °C), the crack propagation speed and fracture toughness under pure mode I and pure mode II increase with increasing the temperature of thermal treatment. While in the second regime (250 to 500 °C), the crack propagation speed and fracture toughness decrease as the temperature increase. The results obtained from granite can be explained by relying on the effect of thermal microcracks presented by Balme, et al. [10]. The growth of thermal microcracks during the heat treatment in the furnace depends mainly on the temperature and the time that the sample is exposed to this temperature. Initially, at temperatures between RT and 250 °C, thermal micro cracks begin to grow and distribute randomly in the material, so their extensions are very limited and do not significantly affect the strength of the grains or the bonds between them. The random distribution of these thermal microcracks around the notch tip greatly obstructs the growth process, causing crack arrest. This obstruction causes an increase in the growing resistance of the fracture. By increasing the temperature of thermal treatment to 500 °C, thermal microcracks extend and form weak planes in the material, which in turn can coalesce with each other under the influence of external loads. For temperatures greater than 500 °C, thermal microcracks extend further to form visible planes of discontinuity as shown in Fig. 3. Our results are qualitatively following the findings of Meredith and Atkinson [41] for the effect of temperature (20 to 400 °C) on the fracture toughness of granite and gabbro. They showed that by increasing the temperature from 20 to 100 °C, fracture toughness of granite and gabbro increases, and then it decreases for T greater than 100 °C. Meredith and Atkinson [41] concluded that the increase of fracture toughness for T between 20 and 100 °C is due to the development of a small number of isolated thermal microcracks. When the fracture tip encounters an isolated thermal microcrack that is unfavorably oriented with respect to the direction of propagating fracture, then the thermal microcrack blunts the fracture tip to grow and a larger crack tip stress intensity is needed to overcome this barrier 'thermal microcrack'. For temperature greater than 100 °C, the density of thermal microcracks increases, and they extend and connect, which facilitate the propagation of fracture tip through these planes of weakness.

5.3.3. Temperature dependence of fracture toughness ratio (K_{IIC}/K_{IC})

The fracture toughness ratio is an important parameter in fracture mechanics to determine the fracture growth of the material and to answer important questions; Is the material resistance to tensile fractures under pure mode I is greater or less than that under pure mode II? Is this ratio affected by heat treatment? Fracture toughness ratio can be determined depending on the analytical fracture criteria such as the maximum tangential stress criterion (σ-criterion, [42]), minimum strain energy density criterion (S-criterion, [43]), and maximum energy release rate criterion (G-criterion, [44]). Erdogan and Sih [42] and Palaniswamy [44] concluded that σ and G criteria fracture toughness under pure mode II is less than that under pure mode I and that the ratio between them K_{IIC}/K_{IC} is 0.866 and 0.627, respectively. Sih [43] indicated that under S-criterion and for plane strain problems, the ratio of fracture toughness is a function of Poisson's ratio (ν) and it is inversely proportional to ν. By increasing Poisson's ratio from 0.0 to 0.5, K_{IIC}/K_{IC} decreases from about 1.22 to 0.0. For Poisson's ratio less than 0.27, S-criterion predicted that K_{IIC} is greater than K_{IC}, while for Poisson's ratio greater than 0.27, the opposite behavior occurred. For Poisson's ratio between 0.25 and 0.37 (most rock types), K_{IIC}/K_{IC} changes between 1.02 and 0.87.

Experimental results of our study in Fig. 10-c show that the fracture toughness ratio in the mudstone and granite is temperature-dependent. By increasing the temperature of thermal treatment from room temperature to 250 and 500 °C, the average value of K_{IIC}/KIC in the mudstone increases from 0.52 to 0.55 and 0.64, respectively, whereas the average value of K_{IIC}/KIC in the granite increases from 0.47 to 0.48 and 0.69, respectively. The increase of K_{IIC}/KIC by increasing the temperature means that the fracture resistance to growth under pure mode II improves better than that under pure mode I. In addition, the K_{IIC}/KIC obtained from this study for mudstone and granite under three temperatures is less than that predicted by the three fracture criteria. Our results agree qualitatively, not quantitatively, with the fracture criteria (σ, G, and S for ν greater than 0.27). This is because the fracture criteria were derived for completely homogeneous materials and do not take the heterogeneous nature and mineralogical composition of the rocks into account.

5.3.4. *Result analysis from the perspective of mineralogical composition*

For two different rock materials under the same thermal treatment condition, significant differences in crack propagation speed, crack acceleration, crack deceleration, and fracture toughness were found. This difference in results depends mainly on the difference in the mineralogical composition of mudstone and granite. As we mentioned earlier, the main constituent mineral of the mudstone is clay (92 %) which has a great affinity for water due to the formation of the diffuse double layer around the negatively charged minerals. Therefore, this mineral is highly affected by thermal treatment due to dehydration and dihydroxylation processes. The main constituent mineral of the granite is plagioclase (70 %) which is not effective with water such as clay. Therefore, the effect of thermal treatment on the results obtained from granite were explained depending on the creation of new thermal microcracks, or extension of preexisting defects such as shown in Fig. 11-b. On the other hand, clays are weak compared to plagioclase and behave in a plastic behavior due to their water absorption property. This also explains the significant difference in results between mudstone and granite.

6. Conclusions

The effect of thermal treatment on two rock types under two loading modes, pure mode I and pure mode II, was investigated experimentally in this study. The first rock type was mudstone which represents clay-rich rocks that have a high affinity for water. The second rock type was granite which does not have water-active minerals. Semi-circular specimens were prepared and thermally treated under temperatures of 250 and 500 °C. To calculate crack propagation speed, crack acceleration, and deceleration, a special electrical circuit was used to determine the cut off time of four copper tapes that were placed on the surface of the SCB specimens. The SCB specimens were then loaded under three points bending test to measure crack propagation speed and fracture toughness under two loading modes. The samples were tested after being thermally treated at three temperatures; RT, 250, and 500 °C. The results of this study can be concluded as follow:

This research showed that for both mudstone and granite and under all temperatures used in this study the area under displacement-load curves under pure mode II is greater than that under pure mode I. Due to this increase in the stored energy the crack propagation speed, crack acceleration, and crack deceleration increased.

It was found that the fracture toughness (K_{IC} and K_{IIC}) in mudstone increase with increasing the temperature from RT to 250 and 500 °C. While in granite, K_{IC} and K_{IIC} increase for T between RT and 250 °C, and then they decrease for T between 250 and 500 °C.

Our results showed that for the three temperatures considered in this work, the crack grows in the mudstone and granite under pure mode I and II through three main stages; the first stage (0 to 5 mm from the notch tip under pure mode I and 0 to 7 mm under pure mode II), the crack accelerates greatly to reach its maximum speed at the first copper tape. During the second stage (5 to 10 mm from the notch tip under pure mode I and 7–14 mm under pure mode II), the crack significantly decelerates to reach a low deceleration third stage (10–15 mm from the notch tip under pure mode I and 14–21 mm under pure mode II).

CRediT authorship contribution statement

Mahmoud Alneasan: Methodology, Software, Validation, Formal analysis, Investigation, Writing – original draft, Visualization. **Abdel Kareem Alzo'ubi:** Conceptualization, Resources, Data curation, Writing – review & editing, Supervision, Project administration, Funding acquisition. **Mahmoud Behnia:** Conceptualization, Supervision, Writing – review & editing. **Omer Mughieda:** Funding acquisition.

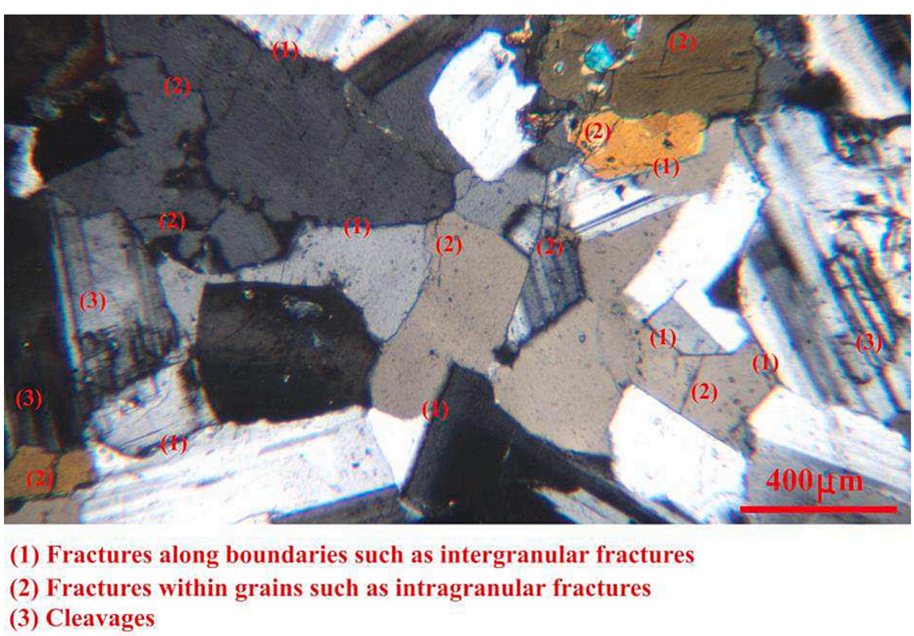

Fig. 11. Different types of fractures observed in granite under the microscope.

Declaration of Competing Interest

The authors declare that they have no known competing financial interests or personal relationships that could have appeared to influence the work reported in this paper.

Acknowledgment

We would like to thank the ORSP at Abu Dhabi University for funding this project (19300529, 19300528). We also would like to extend our thanks to Azmoneh Foulad Consulting Engineers[1] for permission to use facilities in this company's rock mechanics lab under the supervision of Eng. Mohsen Aghababaei[2] and Eng. Behzad Nateghpour[3].

References

[1] A. Alzo'ubi, State of the art, reconstruction of damaged zones: transitory stresses effect and factors controlling rock mass stability, GEOMATE Journal, 14 (2018) 35-43.
[2] M. Behnia, M.C. Seifabad, Stability analysis and optimization of the support system of an underground powerhouse cavern considering rock mass variability, Environm. Earth Sci. 77 (2018) 1–16.
[3] M. Aghababaei, M. Behnia, O. Moradian, Experimental investigation on strength and failure behavior of carbonate rocks under multistage triaxial compression, Int. J. Rock Mech. Min. Sci. 123 (2019), 104099.
[4] M. Behnia, B. Nateghpour, J. Tavakoli, M. Sharifi Broujerdi, Comparison of experimental and empirical methods for estimating the shear strength of rock joints based on the statistical approach, Environm. Earth Sci. 79 (2020) 1–15.
[5] S. Liu, J. Xu, Study on dynamic characteristics of marble under impact loading and high temperature, Int. J. Rock Mech. Min. Sci. 62 (2013) 51–58.
[6] Z. Zhang, J. Yu, S. Kou, P.-A. Lindqvist, Effects of high temperatures on dynamic rock fracture, Int. J. Rock Mech. Min. Sci. 38 (2001) 211–225.
[7] T. Funatsu, M. Seto, H. Shimada, K. Matsui, M. Kuruppu, Combined effects of increasing temperature and confining pressure on the fracture toughness of clay bearing rocks, Int. J. Rock Mech. Min. Sci. 41 (2004) 927–938.
[8] N. Al-Shayea, K. Khan, S. Abduljauwad, Effects of confining pressure and temperature on mixed-mode (I–II) fracture toughness of a limestone rock, Int. J. Rock Mech. Min. Sci. 37 (2000) 629–643.
[9] P. Kang, L. Hong, Y. Fazhi, Z. Quanle, S. Xiao, L. Zhaopeng, Effects of temperature on mechanical properties of granite under different fracture modes, Eng. Fract. Mech. 226 (2020), 106838.
[10] M. Balme, V. Rocchi, C. Jones, P. Sammonds, P. Meredith, S. Boon, Fracture toughness measurements on igneous rocks using a high-pressure, high-temperature rock fracture mechanics cell, J. Volcanol. Geoth. Res. 132 (2004) 159–172.
[11] J.-P. Zuo, H.-P. Xie, F. Dai, Y. Ju, Three-point bending test investigation of the fracture behavior of siltstone after thermal treatment, Int. J. Rock Mech. Min. Sci. 70 (2014) 133–143.
[12] B. Mahanta, T. Singh, P. Ranjith, Influence of thermal treatment on mode I fracture toughness of certain Indian rocks, Eng. Geol. 210 (2016) 103–114.
[13] M.R. Chandler, P.G. Meredith, N. Brantut, B.R. Crawford, Effect of temperature on the fracture toughness of anisotropic shale and other rocks, Geological Society, London, Special Publications 454 (2017) 295–303.
[14] Z. Chen, X. Jin, M. Wang, A new thermo-mechanical coupled DEM model with non-spherical grains for thermally induced damage of rocks, J. Mech. Phys. Solids 116 (2018) 54–69.
[15] E. Veveakis, S. Alevizos, I. Vardoulakis, Chemical reaction capping of thermal instabilities during shear of frictional faults, J. Mech. Phys. Solids 58 (2010) 1175–1194.
[16] K.T. Chau, J.-F. Shao, Subcritical crack growth of edge and center cracks in façade rock panels subject to periodic surface temperature variations, Int. J. Solids Struct. 43 (2006) 807–827.
[17] R. Liu, Z. Zhu, Y. Li, B. Liu, D. Wan, M. Li, Study of rock dynamic fracture toughness and crack propagation parameters of four brittle materials under blasting, Eng. Fract. Mech. 225 (2020), 106460.
[18] B. Liu, Z. Zhu, R. Liu, L. Zhou, D. Wan, Study on the Fracture Behavior of Cracks Emanating from Tunnel Spandrel under Blasting Loads by Using TMCSC Specimens, Shock Vib. 2019 (2019) 1–13.
[19] D. Wan, Z. Zhu, R. Liu, B. Liu, J. Li, Measuring method of dynamic fracture toughness of mode I crack under blasting using a rectangle specimen with a crack and edge notches, Int. J. Rock Mech. Min. Sci. 123 (2019), 104104.
[20] M. Alneasan, M. Behnia, Strain rate effects on the crack propagation speed under different loading modes (I, II and I/II): Experimental investigations, Eng. Fract. Mech. 258 (2021) 108118.
[21] M.D. Kuruppu, Y. Obara, M.R. Ayatollahi, K. Chong, T. Funatsu, ISRM-suggested method for determining the mode I static fracture toughness using semi-circular bend specimen, Rock Mech. Rock Eng. 47 (2014) 267–274.
[22] L. Griffiths, M. Heap, P. Baud, J. Schmittbuhl, Quantification of microcrack characteristics and implications for stiffness and strength of granite, Int. J. Rock Mech. Min. Sci. 100 (2017) 138–150.
[23] P. Glover, P. Baud, M. Darot, P. Meredith, S. Boon, M. LeRavalec, S. Zoussi, T. Reuschlé, α/β phase transition in quartz monitored using acoustic emissions, Geophys. J. Int. 120 (1995) 775–782.
[24] M. Alneasan, M. Behnia, An experimental investigation on tensile fracturing of brittle rocks by considering the effect of grain size and mineralogical composition, Int. J. Rock Mech. Min. Sci. 137 (2021), 104570.
[25] S.L. Crouch, A.M. Starfield, F. Rizzo, Boundary element methods in solid mechanics, (1983).
[26] M. Behnia, K. Goshtasbi, M. Fatehi Marji, A. Golshani, The effect of layers elastic parameters on hydraulic fracturing propagation utilizing displacement discontinuity method, J. Anal. Numer. Methods Min. Eng. 2 (2012) 1–13.
[27] M. Alneasan, M. Behnia, R. Bagherpour, Analytical and numerical investigations of dynamic crack propagation in brittle rocks under mixed mode loading, Constr. Build. Mater. 222 (2019) 544–555.
[28] M.R. Ayatollahi, M.R.M. Aliha, M.M. Hassani, Mixed mode brittle fracture in PMMA—an experimental study using SCB specimens, Mater. Sci. Eng., A 417 (1-2) (2006) 348–356.
[29] D. Cook, Calcined clay, shale and other soils, in: R.N. Swamy (Ed.), Cement RepläCement Materials, Surrey University Press, London, 1986, pp. 40–72.
[30] R. Snellings, G. Mertens, J. Elsen, Supplementary cementitious materials, Rev. Mineral. Geochem. 74 (1) (2012) 211–278.
[31] A. Alzo'ubi, Numerical simulation of mechanical movement of layered rock slopes, in: ISRM International Symposium-8th Asian Rock Mechanics Symposium, OnePetro, 2014.
[32] K. Arakawa, T. Mada, K. Takahashi, Correlations among dynamic stress intensity factor, crack velocity and acceleration in brittle fracture, Int. J. Fract. 105 (2000) 311–320.
[33] K. Takahashi, K. Arakawa, Dependence of crack acceleration on the dynamic stress-intensity factor in polymers, Exp. Mech. 27 (1987) 195–199.
[34] K. Arakawa, K. Takahashi, Relationships between fracture parameters and fracture surface roughness of brittle polymers, Int. J. Fract. 48 (1991) 103–114.
[35] B.N. Whittaker, R.N. Singh, G. Sun, Rock fracture mechanics, Principles, Des. Appl. (1992).
[36] T. Tamilselvan, K. Lo, Y. Gong, M. Lai, A study of Mode II fracture toughness test standardisation of metals. In: 10th International Congress of Fracture, 2001.
[37] D. Smith, M. Ayatollahi, M. Pavier, The role of T-stress in brittle fracture for linear elastic materials under mixed-mode loading, Fatigue Fract. Eng. Mater. Struct. 24 (2001) 137–150.
[38] M. Monsif, A. Zerouale, N. Idrissi Kandri, M. Mozzon, P. Sgarbossa, F. Zorzi, F. Tateo, S. Tamburini, E. Franceschinis, S. Carturan, R. Bertani, Chemical-physical and mineralogical characterization of ceramic raw materials from Moroccan northern regions: Intriguing resources for industrial applications, Appl. Clay Sci. 182 (2019) 105274.
[39] G. Cultrone, F.J.C. Rosua, Growth of metastable phases during brick firing: Mineralogical and microtextural changes induced by the composition of the raw material and the presence of additives, Appl. Clay Sci. 185 (2020), 105419.
[40] E. Escalera, M.L. Antti, M. Odén, Thermal treatment and phase formation in kaolinite and illite based clays from tropical regions of Bolivia, in, IOP Conf. Ser. Mater. Sci. Eng. IOP Publishing 31 (2012) 012017.
[41] P. Meredith, B. Atkinson, Fracture toughness and subcritical crack growth during high-temperature tensile deformation of Westerly granite and Black gabbro, Phys. Earth Planet. Inter. 39 (1985) 33–51.
[42] F. Erdogan, G. Sih, On the crack extension in plates under plane loading and transverse shear, (1963).
[43] G.C. Sih, Strain-energy-density factor applied to mixed mode crack problems, Int. J. Fract. 10 (1974) 305–321.
[44] K. Palaniswamy, Crack propagation under general in-plane loading, in, California Institute of Technology, 1972.

[1] https://en.azmouneh.com/.
[2] m.aghababaei@mi.iut.ac.ir.
[3] b.nateghpour@mi.iut.ac.ir.